# Simultaneous Inhibition and Redistribution of Spontaneous Light Emission in Photonic Crystals

**Masayuki Fujita, Shigeki Takahashi, Yoshinori Tanaka, Takashi Asano, Susumu Noda***

**Inhibiting spontaneous light emission and redistributing the energy into useful forms are desirable objectives for advances in various fields, including photonics, illuminations, displays, solar cells, and even quantum-information systems. We demonstrate both the "inhibition" and "redistribution" of spontaneous light emission by using two-dimensional (2D) photonic crystals, in which the refractive index is changed two-dimensionally. The overall spontaneous emission rate is found to be reduced by a factor of 5 as a result of the 2D photonic bandgap effect. Simultaneously, the light energy is redistributed from the 2D plane to the direction normal to the photonic crystal.**

Spontaneous light emission is a fundamental factor (or bottleneck) limiting the performance of devices in various fields, including photonics (*1*), illuminations (*2*), displays (*3*), solar cells (*4*), and quantum-information systems (*5*). For example, in light-emitting diodes, spontaneous emission that is not extracted from the device contributes to losses. Similarly, in lasers, spontaneous emission that does not couple to the lasing mode results in both losses and noise. Therefore, inhibiting undesirable spontaneous light emission and redistributing (*6*) the energy into useful forms will allow advances in these fields. Three-dimensional (3D) photonic crystals (*7–13*), which have a 3D periodic refractive-index distribution that eliminates the optical modes in all 3D directions via the photonic bandgap (PBG) effect, have been used to demonstrate the inhibition of spontaneous light emission (*11*, *13*). However, redistribution of the energy has yet to be demonstrated.

Here, we investigate both the "inhibition" and "redistribution" of spontaneous light emission using 2D photonic crystals (*14–19*). These crystals are predicted to provide a mechanism for controlling spontaneous emission, which reflects their 2D nature (*14*): The overall spontaneous emission rate is expected to decrease as a result of the inhibition of optical modes in all 2D directions by the 2D PBG effect, whereas the emission efficiency for the direction normal to the crystal (in which the 2D PBG effect does not appear) should increase via redistribution of the saved energy. Although an experimental trial has been reported recently (*20*), it is not clear whether the spontaneous emission is inhibited by the 2D PBG effect.

Spontaneous emission originates from fluctuations in the vacuum field. Under a weak light–matter coupling regime, the rate of spontaneous emission ($R_{spon}$) is given by Fermi's golden rule (*21*) and is determined by the number of optical modes. In order to control spontaneous light emission, the optical modes must therefore be manipulated. Figure 1 shows the 2D photonic crystal used, in which a triangular-lattice 2D photonic crystal is formed in a semiconductor (GaInAsP) slab. The structure incorporates a single quantum well (QW) as the light-emitting material, emitting light with a transverse-electric (TE) polarization in which the dipole moment is orientated parallel to the slab plane (*22*). The optical modes in the thin slab can be categorized into two modes: "slab modes," which are confined to

Department of Electronic Science and Engineering, Kyoto University, Katsura, Nishikyo-Ku, Kyoto 615-8510, Japan.

*To whom correspondence should be addressed. E-mail: snoda@kuee.kyoto-u.ac.jp

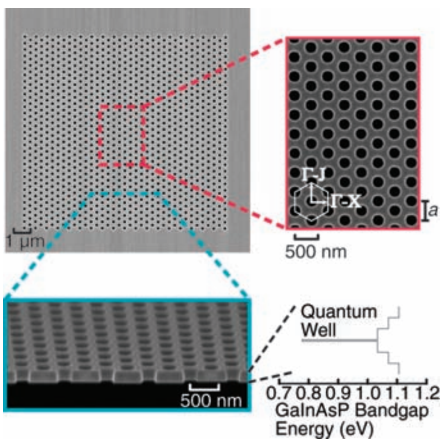


**Fig. 1.** The semiconductor (GaInAsP) 2D photonic-crystal slab. A scanning electron micrograph is shown. The 2D photonic-crystal slab has a triangular lattice structure with an air-hole radius *r* of 0.29*a* (lattice constant *a* = 300 to 500 nm) and a thickness of 245 nm. A 5-nm-wide single QW is inserted at the center of the slab to form the light-emitting layer.

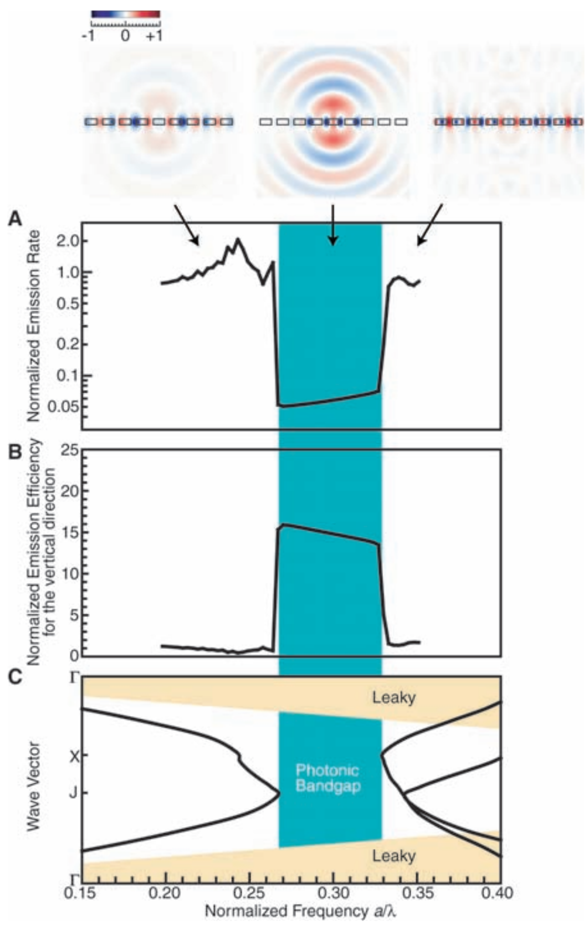


**Fig. 2.** Theoretical analyses of the effects of the 2D photonic-crystal slab (Fig. 1) on spontaneous-emission inhibition and energy redistribution. A flat semiconductor (GaInAsP) slab on a semiconductor (InP) substrate is used as a reference. The refractive index and thickness of the semiconductor slab are 3.27 and 0.6*a*, respectively. The refractive index of the substrate and air are 3.13 and 1.0, respectively. (**A**) Calculated spontaneous emission rate as a function of frequency, normalized by the result calculated for the reference structure. (**B**) Emission efficiency in the vertical direction for various frequencies, normalized by the results calculated for the reference. (Top) Schematic views illustrate how emission is controlled by the 2D PBG effect. The arrow denotes the corresponding frequency region. (**C**) Photonic-band diagram calculated by 3D FDTD using periodic boundary conditions. The solid lines show the dispersion relation of the 2D slab modes. The frequency region between 0.267 and 0.330 corresponds to the 2D PBG region. "Leaky" refers to the region in which the TIR condition is not satisfied and light is emitted outside the crystal surface.

the 2D plane by satisfying the total internal reflection (TIR) condition for the vertical direction, and "vertical modes," which do not satisfy the TIR condition and are emitted outside the slab. Excited carriers that are confined in the QW generate spontaneous emission coupled to both slab and vertical modes, and the spontaneous emission rate ($R_{spon}$) can be expressed by

$$R_{spon} = R_{slab} + R_{vertical} \quad (1)$$

Here, $R_{slab}$ and $R_{vertical}$ denote the spontaneous emission rate for slab modes and vertical modes, respectively. For a semiconductor slab with a large refractive index that is surrounded by low–refractive index air cladding (Fig. 1), light is strongly confined within the slab, and the condition $R_{slab} \gg R_{vertical}$ is satisfied. Therefore, spontaneous emission from the QW is mostly coupled to the slab modes. However, when a 2D photonic-crystal structure is incorporated in the slab, $R_{slab}$ is expected to be strongly reduced, whereas basically no modification of $R_{vertical}$ occurs. As a result, a marked reduction in $R_{spon}$ is expected through the reduction of $R_{slab}$. The 2D PBG is responsible for inhibiting emission into the slab modes so that photons emitted from the QW can only couple into the vertical modes. Therefore, the efficiency of spontaneous emission in the vertical direction, which can be detected, will increase. These two effects—the reduction of $R_{spon}$ due to the inhibition of spontaneous emission into 2D slab modes within the PBG and the increased emission efficiency of the vertical modes—will occur simultaneously. This implies that the 2D photonic crystal effectively redistributes the light energy from the 2D plane to the vertical direction.

We quantitatively investigated the spontaneous emission modification and energy redistribution within the 2D photonic-crystal structure. For these purposes, we calculated the spontaneous emission rate and the emission efficiency in the vertical direction using the 3D finite-difference time-domain (FDTD) method (*23*, *24*) and normalized the results using values calculated for an equivalent structure without a photonic crystal. The details of the FDTD calculation are described in the supporting text (*25*). Figure 2, A and B, show the results, and Fig. 2C illustrates the corresponding photonic band diagram for the 2D photonic-crystal slab. Figure 2A shows that the spontaneous emission rate is reduced by more than a factor of 15 within the PBG region (blue region) compared with that outside the PBG region. Simultaneously, the emission efficiency for the direction normal to the crystal (Fig. 2B) increases by more than a factor of 15 within the PBG region compared with that outside the PBG region. Schematic views of the cross-sectional electric field on such situations are shown also in Fig. 2, where a dipole oscillator is placed at one point on the slab and is continuously excited so that the total power emitted in all directions becomes constant for each case. When the emission wavelength is outside the PBG, emission normal to the crystal is weak because $R_{slab} \gg R_{vertical}$ and the energy is distributed mostly in the 2D slab modes. However, when the wavelength is within the PBG, emission normal to the crystal is increased notably, despite the small value of $R_{vertical}$, because emission into 2D slab modes is inhibited ($R_{slab} \sim 0$) and the energy is redistributed into vertical emission modes.

Our samples were fabricated using a combination of epitaxial growth, electron-beam lithography, plasma etching, and chemical etching (*26*). A series of samples were prepared on the same wafer, with the lattice constants $a$ ranging from 300 to 500 nm in 10-nm intervals, in order to investigate a wide normalized-frequency range. The samples were optically pumped using a Ti-$Al_2O_3$ laser emitting at 980 nm with a pulse width of 2 ps and a repetition frequency of 2 MHz. The PBG region was at first estimated for each sample under a sufficiently strong excitation condition (10 W/cm$^2$ on average) (*27*). Then, the average laser power was reduced to 0.5 W/cm$^2$ so that only recombination processes in the QW involving emission of TE polarized light could occur, in order to satisfy the assumption made in the calculation. If the optical absorption coefficient of the slab is assumed to be $2 \times 10^4$ cm$^{-1}$, the excited-carrier density is estimated as $\sim 8 \times 10^{17}$ cm$^{-3}$. Under the weak excitation condition, time-integrated emission spectra (Fig. 3A), which indicate the emission efficiency in the vertical direction, were measured at 4 K using a multichannel GaInAs detector system. Then, time-resolved emission measurements (Fig. 3B) were made at the same temperature using a time-correlated single-photon-counting system (*28*) incorporating a photomultiplier detector, where we collected spectra across the whole emission wavelength range, in order to measure the overall emission rate.

When the emission wavelength is within the PBG region (Fig. 3, A and B) ($a$ = 390 to 480 nm), the spontaneous emission lifetime (which corresponds to $1/R_{spon}$) increases compared with that observed in structures not incorporating photonic crystals. Simultaneously, the emission efficiency increases in the direction normal to the crystal compared with that in structures not incorporating photonic crystals. In contrast, when the emission wave-

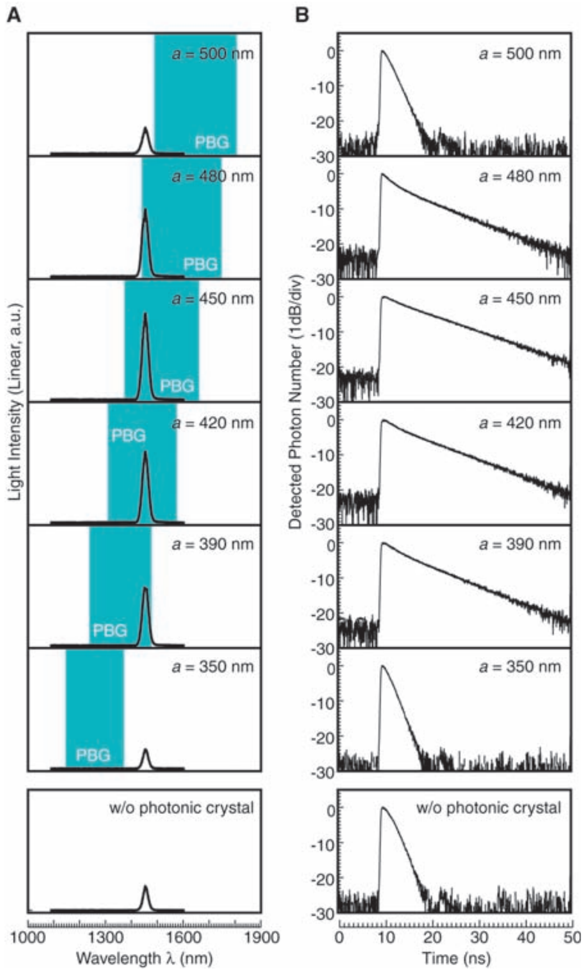


**Fig. 3.** Experimental results. (**A**) Time-integrated emission spectra for samples with a range of lattice constants between 350 and 500 nm. The blue cross-hatching denotes the PBG region. (**B**) Time-resolved photoluminescence measurements for various samples. When the spontaneous-emission spectrum lies within the PBG region, the emission lifetime increases by a factor of 5 relative to that observed when the spectrum lies outside the PBG region (and compared with that of the sample without a photonic-crystal structure). A corresponding increase in the light-emission efficiency in the vertical direction, where the PBG effect does not occur, is clearly observed in the PBG region, as seen in (A).

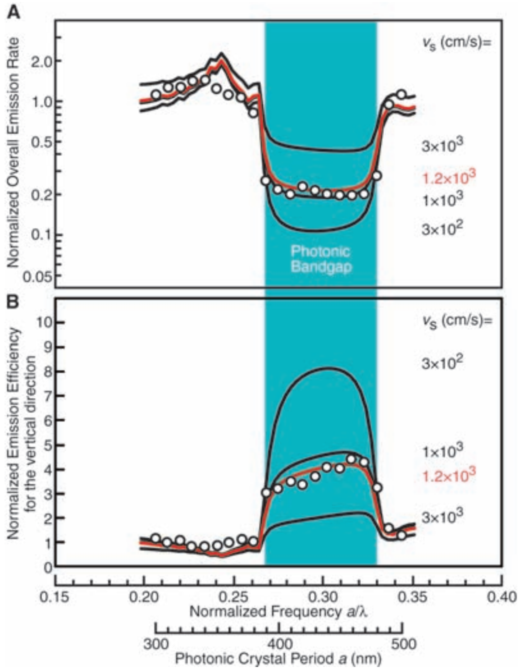


**Fig. 4.** Plots of the experimental results for a wide range of normalized frequencies (open circles). (**A**) Overall spontaneous-emission decay rates. (**B**) Emission efficiency in the direction normal to the crystal. The results were normalized by those for the reference sample without photonic crystals. The solid lines represent theoretically fitted results for a range of values of $v_s$. The experimentally observed inhomogeneous broadening of the emission spectra is accounted for in the calculation. The closest correspondence between the experimental results and theoretical curves is obtained for $v_s = 1.2 \times 10^3$ cm/s.

length lies outside the PBG (Fig. 3, A and B) ($a$ = 350 and 500 nm), the spontaneous emission lifetime and the emission efficiency in the normal direction are both comparable to those observed in structures without photonic crystals. Figure 4 summarizes these results over a range of normalized frequencies (open circles) with the emission lifetimes converted to corresponding emission rates. The 2D PBG effect is clearly seen in Fig. 4A. The overall emission rate decreases by a factor of 5 within the PBG region compared with those outside the PBG region, and the increase in emission efficiency in the direction normal to the crystal is clearly seen in Fig. 4B. These results are in good agreement with the theoretical analyses shown in Fig. 2. Therefore, simultaneous inhibition and redistribution of spontaneous emission are successfully demonstrated by this experiment.

We also fitted the experimental results more quantitatively by considering the energy loss due to nonradiative recombination of excited carriers in the QW layer. Surface recombination is the most likely mechanism for nonradiative relaxation, and the rate ($R_{non}$) is proportional to the ratio of the exposed QW surface area ($S_w$) to its overall volume ($V_w$) (*22*), which is expressed as

$$R_{non} = \frac{S_w}{V_w} v_s = \frac{4\pi r}{\sqrt{3}a^2 - 2\pi r^2} v_s \qquad (2)$$

Here, $v_s$ is the surface-recombination velocity and $r$ is the air-hole radius. The total recombination rate ($R_T$) is therefore expressed as

$$R_T = R_{spon} + R_{non} \qquad (3)$$

The experimentally observed rate should be proportional to $R_T$. Similarly, the emission efficiency for the direction normal to the photonic crystal can be modified in light of this nonradiative recombination process. Under these conditions, the experimental results can be fitted, as shown in Fig. 4, A and B. Lines have been drawn for various values of $v_s$. There is good agreement between the theoretical calculation and the experimental results for $v_s = 1.2 \times 10^3$ cm/s. This is a factor of 10 lower than typical values for GaInAsP (*22*) at room temperature and is consistent with the effects of sample cooling. We believe that similar values of $v_s$ will be attainable at room temperature, with special treatment of the surface (*29*). The use of high-quality crystalline silicon, with surface-recombination velocities of less than 1 cm/s (*30*), might also be advantageous for the suppression of nonradiative processes, because it will lead to the realization of high-quality silicon-based photonic devices. Furthermore, applications for the control of thermal (or black body) emission would no longer be affected by surface-recombination processes.

We believe that our demonstration of simultaneous inhibition and redistribution of spontaneous light emission in photonic crystals is an important step toward the evolution of photonic devices and systems in various fields, including photonics, illuminations, displays, solar cells, and even quantum-information systems.

### References and Notes


1. B. E. A. Saleh, M. C. Teich, *Fundamentals of Photonics* (Wiley, New York, 1991).
2. D. A. Steigerwald *et al.*, *IEEE J. Sel. Top. Quantum Electron.* **8**, 310 (2002).
3. K. Ziemelis, *Nature* **399**, 408 (1999).
4. M. Grätzel, *Nature* **414**, 338 (2001).
5. H. Mabuchi, A. C. Doherty, *Science* **298**, 1372 (2002).
6. The term "redistributing" is used here to indicate that the energy, which is otherwise utilized (or distributed) for undesirable spontaneous emission, is (re)distributed in more useful forms. In light-emitting diodes, this energy, which is otherwise distributed in spontaneous emission that cannot be extracted from a device, is (re)distributed in emission that can be extracted from the device. In lasers, the energy is redistributed into the lasing mode. In solar cells, the energy is redistributed for use as electrical energy.
7. E. Yablonovitch, *Phys. Rev. Lett.* **58**, 2059 (1987).
8. S. John, *Phys. Rev. Lett.* **58**, 2486 (1987).
9. S. Noda, K. Tomoda, N. Yamamoto, A. Chutinan, *Science* **289**, 604 (2000).
10. A. Blanco *et al.*, *Nature* **405**, 437 (2000).
11. S. Ogawa, M. Imada, S. Yoshimoto, M. Okano, S. Noda, *Science* **305**, 227 (2004).
12. M. Qi *et al.*, *Nature* **429**, 538 (2004).
13. P. Lodahl *et al.*, *Nature* **430**, 654 (2004).
14. S. Fan, P. R. Villeneuve, J. D. Jonnopoulos, *Phys. Rev. Lett.* **78**, 3294 (1997).
15. O. Painter *et al.*, *Science* **284**, 1819 (1999).
16. M. Boroditsky *et al.*, *J. Lightwave Technol.* **17**, 2096 (1999).
17. S. Noda, A. Chutinan, M. Imada, *Nature* **407**, 608 (2000).
18. S. Noda, Y. Yokoyama, M. Imada, A. Chutinan, M. Mochizuki, *Science* **293**, 1123 (2001).
19. Y. Akahane, T. Asano, B. S. Song, S. Noda, *Nature* **425**, 944 (2003).
20. H. Y. Ryu, Y. H. Lee, R. Sellin, D. Bimberg, *Appl. Phys. Lett.* **79**, 3573 (2001).
21. R. Loudon, *The Quantum Theory of Light* (Oxford Univ. Press, New York, 2000).
22. L. A. Coldren, S. W. Corzine, *Diode Lasers and Photonic Integrated Circuits* (Wiley, New York, 1995), pp. 148–153, 518–525.
23. J. K. Hwang, H. Y. Ryu, Y. H. Lee, *Phys. Rev. B* **60**, 4688 (1999).
24. R. K. Lee, Y. Xu, A. Yariv, *J. Opt. Soc. Am. B* **17**, 1438 (2000).
25. The details of the FDTD method are presented as supporting material on *Science* Online.
26. M. Fujita, A. Sugitatsu, T. Uesugi, S. Noda, *Jpn. J. Appl. Phys. Part 2* **43**, L1400 (2004).
27. The PBG region is identified as follows. At the edges of the PBG (the upper and lower boundaries of the PBG region), the group velocity of light approaches zero and waves propagating in different directions in the slab couple in a type of 2D cavity resonator, resulting in standing-wave formation. Under sufficiently strong excitation, above the population-inversion threshold, a resonant peak is observed at the photonic band edge as a result of stimulated emission. In these experiments, we used an excitation intensity of 10 W/cm², which is 20 times as high as that used in the spontaneous emission-lifetime measurement, to obtain such a population inversion. In this way, we detected resonant peaks corresponding to the photonic band edges over a broad wavelength range. It was possible to fit the relation between the band-edge wavelength and the photonic-crystal period using a linear function, obtaining $\lambda_S = 2.28a + 350$ (nm) for the shorter wavelength band edge and $\lambda_L = 2.90a + 357$ (nm) for the longer wavelength band edge. These results are consistent with the 3D FDTD photonic band-diagram calculation.
28. D. O' Connor, D. Phillips, *Time-Correlated Single Photon Counting* (Academic Press, London, 1985).
29. E. Yablonovitch, C. J. Sandroff, R. Bhat, T. Gmitter, *Appl. Phys. Lett.* **51**, 439 (1987).
30. E. Yablonovitch, D. L. Allara, C. C. Chang, T. Gmitter, T. B. Bright, *Phys. Rev. Lett.* **57**, 249 (1986).


31. This work was partly supported by a Grant-in-Aid (no. 15GS0209) and an IT project grant from the Ministry of Education, Culture, Sports, Science and Technology of Japan, and by the Japan Science and Technology Corporation (CREST). M.F. was supported by a Research Fellowship of the Japan Society for the Promotion of Science (no. 15004417).


**Supporting Online Material**
www.sciencemag.org/cgi/content/full/308/5726/1296/DC1
SOM Text
Figs. S1 and S2
References and Notes


31 January 2005; accepted 4 April 2005
10.1126/science.1110417

# Simultaneous Inhibition and Redistribution of Spontaneous Light Emission in Photonic Crystals

Masayuki Fujita, Shigeki Takahashi, Yoshinori Tanaka, Takashi Asano, and Susumu Noda

*Science*, 308 (5726), • DOI: 10.1126/science.1110417